

Comparison of laser cooling of the lattice of wide-band-gap semiconductors using nonlinear or linear optical excitations

T. Apostolova, Danhong Huang, P. M. Alsing, and D. A. Cardimona

Air Force Research Laboratory, Space Vehicles Directorate, Kirtland Air Force Base, New Mexico 87117, USA

(Received 29 April 2004; revised manuscript received 9 August 2004; published 13 January 2005)

A generalized nonlocal energy-balance equation for excited carriers and phonons is established for studying the laser cooling of a lattice of a wide-band-gap semiconductor such as AlN using a He-Ne laser through a three-photon nonlinear excitation process. The power-exchange densities of the system are calculated and compared for different strengths of the excitation field. When the power-exchange density is positive, it implies laser cooling of the lattice. The effects of initial lattice temperature and field-frequency detuning on the laser-cooling phenomenon under the three-photon nonlinear excitation process are described. The power-exchange densities are compared for both laser cooling and heating using linear and nonlinear excitations. We find that the linear excitation seems more favorable than the nonlinear excitation for laser cooling. However, the resonant three-photon nonlinear absorption will allow us the use of a common He-Ne laser for laser cooling of the lattice in AlN, rather than a more expensive ultraviolet laser.

DOI: 10.1103/PhysRevA.71.013810

PACS number(s): 42.50.Ct, 32.80.Pj, 42.65.-k, 42.50.Nn

I. INTRODUCTION

Laser cooling of the lattice in solids and semiconductors is a topic of intense, ongoing theoretical and experimental investigation [1–5]. The best semiconductor materials and the optimal conditions for achieving laser cooling are still to be determined. In a previous paper [6], we established a nonlocal theory on a microscopic level which provided an evolution equation for the lattice temperature by including dynamical effects. This theory established the criteria for the occurrence and efficiency of laser cooling of a semiconductor lattice and gave important qualitative predictions. It was found that semiconductors with a large band gap are expected to achieve a high laser-cooling efficiency due to their short radiative decay time [7]. However, the frequency of the laser field required to produce a linear excitation of electrons and holes falls into the ultraviolet regime. There are very few available laser sources in this frequency range. If a nonlinear excitation scheme could be used, e.g., resonant three-photon nonlinear absorption [8], the frequency of a pump laser would then fall into the range of the He-Ne laser (with photon energy of 1.96 eV).

We are aware of the fact that multiphoton absorption in bulk semiconductors with photon energy smaller than the band gap is generally a weak process and difficult to observe. However, it is still observable experimentally [9] for two-photon absorption in GaAs quantum wires. In addition, there have been a lot of theoretical studies that referred to the effect of multiphoton absorption in semiconductors on the second- [10] and third-order susceptibility [11].

The nonlinear excitation laser-cooling process of interest in this paper is as follows. The application of a strong laser field first excites electrons from the valence band edge to the conduction band edge via resonant three-photon nonlinear absorption, producing cold conduction electrons and valence holes in a bulk semiconductor. Within several hundred femtoseconds following the initial photoexcitation, ultrafast carrier-carrier scattering and carrier-phonon scattering modi-

fied by the strong laser field will heat the cold excited carriers by taking thermal energy from the lattice [12]. As a result, a quasiequilibrium Fermi-Dirac distribution of carriers is established in about 0.1 ps, with a carrier temperature determined by the intensity and frequency of the excitation field, as well as by the initial lattice temperature [13]. After a few tens of nanoseconds, radiative recombination of the excited carriers begins [7]. Due to ultrafast carrier-phonon scattering following the nonlinear excitation, spontaneous photons with energies higher than the input energy of the three pump photons can be emitted, allowing the lattice to cool.

The conservation of the total energy of carriers, phonons, and spontaneous photons is assumed due to ultrafast carrier scattering with phonons. It forms the basis of our application of the energy-balance equation to electrons and holes in this paper. However, the energy of the phonon system interacting with carriers due to vibration of the thermally isolated lattice cannot be balanced by thermal radiation from the surroundings. As a result, the lattice temperature drops with time due to transferring of net energy to electrons and holes. At the same time, the energy-balance equation at a reduced lattice temperature quickly drives the carrier temperature to a new, lower quasiequilibrium value.

Using a generalized nonlocal energy-balance equation for the excited carriers, we study the possibility for the laser cooling of the lattice of a wide-band-gap semiconductor such as AlN using photons from a He-Ne laser through the above nonlinear excitation process. In this work, we further investigate the conditions for laser cooling of the lattice by exploring the effect of nonlinear excitation on the laser cooling and comparing it with the case for linear laser cooling. From our comparison, we find that the linear excitation scheme seems more favorable for laser cooling of the lattice. However, photon sources with ultraviolet frequencies are required to excite carriers in the linear excitation case while a He-Ne laser can be used for the nonlinear excitation case. The advantage of using nonlinear excitation is that it allows us to use a different range of photon energies for achieving laser cooling of

the lattice of a wide-band-gap semiconductor although it is not as efficient as laser cooling using single-photon excitation.

The organization of this paper is as follows. In Sec. II we establish our model and theory. Numerical results and discussions are presented in Sec. III for photoexcited carrier concentrations and power-exchange densities of carriers with phonons and photons for the linear and nonlinear excitation cases. The paper is briefly concluded in Sec. IV.

II. MODEL AND THEORY

Our laser-cooling model consists of three successive steps. First, a cold electron is pumped coherently by a laser beam from the top of the valence band to the bottom of the conduction band. Next, the induced carriers are heated to higher energy levels via intraband inelastic phonon scattering. The carrier distributions change from coherent ones to quasiequilibrium ones, while the photoexcited carrier density is kept constant. Lastly, the hot electron spontaneously decays to give rise to a photon, thus subtracting from the material a power amount larger than that gained by the pump process.

After electrons are excited by an external electromagnetic field from a lower valence band to an upper conduction band in a semiconductor, ultrafast intraband electron-electron, electron-phonon, and electron-impurity scattering will redistribute the electrons within the conduction band giving rise to a quasiequilibrium Fermi-Dirac distribution in the conduction band with an electron temperature T_e different from the lattice temperature T_L . For a wide-band-gap semiconductor such as AlN (with a bandgap 6.3 eV), we need to use two- or three-photon nonlinear absorption processes for the creation of photoexcited electrons and holes if we are limited to the use of visible lasers (with photon energies ranging from 1.6 to 3.1 eV). In the presence of three-photon nonlinear laser absorption, we use a perturbative density-matrix theory [8,14] and keep only the resonant three-photon nonlinear absorption. This gives rise to the excited carrier concentration for coherent three-photon excitation as a result of a perturbative treatment of the steady-state density-matrix theory due to the balance between the optical gain and the optical absorption in the absence of carrier scattering and photoluminescence, as is the case in the first step [8,14]

$$n_e = n_h = \frac{1}{4\pi^2} \left(\frac{2\mu}{\hbar^2} \right)^{3/2} \int_0^\infty dx \sqrt{x} \times \left\{ 1 - \frac{|x + E_G - 3\hbar\Omega_p|}{[(x + E_G - 3\hbar\Omega_p)^2 + 4\Delta_0^2(x)]^{1/2}} \right\}, \quad (1)$$

where $x = \hbar^2 k^2 / 2\mu$, k is the wave number of carriers, n_α is the concentration of electrons ($\alpha=e$) or holes ($\alpha=h$), E_G is the band gap of the host semiconductor, Ω_p is the angular frequency of the excitation field, and $1/\mu = 1/m_e^* + 1/m_h^*$ with m_e^* (m_h^*) being the effective mass of electrons (holes). The field-broadening effect in Eq. (1) is found to be [8]

$$\Delta_0^2(x) = \frac{4\Delta_R^6}{[(E_G + x)^2 - \hbar^2\Omega_p^2]^2}, \quad (2)$$

and $2\Delta_R$ is the Rabi splitting which is given by [15]

$$\Delta_R^2 = \frac{e^2 \mathcal{E}_p^2}{2m_0\Omega_p^2} \left(\frac{m_0}{m_e^*} - 1 \right) \frac{E_G(E_G + \delta_0)}{2(E_G + 2\delta_0/3)}, \quad (3)$$

where \mathcal{E}_p is the amplitude of the excitation field, δ_0 is the spin-orbit splitting of the semiconductor, and m_0 is the free-electron mass. For medium- to wide-band-gap semiconductors at low temperatures and low carrier concentrations, thermal excitation of carriers, impact ionization, and Auger recombination can be neglected due to the large band gap. Moreover, due to ultrafast electron-electron and electron-phonon scattering, the distributions of carriers $f_k^{e,h}$ are assumed to be Fermi-Dirac functions for electrons and holes, respectively. The exciton effect has been ignored because the exciton binding energy $(\hbar^2/2\mu a_B^2) \exp(-2\Lambda_{eh} a_B)$ is small compared to the thermal energy due to screening by photoexcited carriers [16], where $a_B = 4\pi\epsilon_0\epsilon_r\hbar^2/\mu e^2$ is the effective Bohr radius and $1/\Lambda_{eh}$ is the Thomas-Fermi screening length [17,18] with $\Lambda_{eh}^2 = 4\sqrt{m_e^* m_h^*} (3\pi^2 n_e)^{1/3} / \pi\mu a_B$.

In general, the power gain by electrons from the absorption of the excitation field cannot be balanced by the power loss due to spontaneous photon emission. As a result, electrons either take energy from or give energy to phonons through inelastic scattering, depending on the sign of the difference between the electron temperature and the lattice temperature. The electron temperature can be determined by a generalized nonlocal energy-balance equation for any given lattice temperature. Electron-phonon scattering greatly contributes to the nonlocal energy-balance equation.

The formula for the photoluminescence power in the third step can be derived from a standard many-body theory [see [19] and Refs. [22,23] therein]. The power-density loss due to spontaneous photon emission is [16,19,20]

$$\mathcal{W}_{sp} = \frac{\sqrt{\epsilon_r} e^2}{2\pi^3 \hbar^2 m_0 \epsilon_0 c^3} \left(\frac{m_0}{m_e^*} - 1 \right) \frac{E_G(E_G + \delta_0)}{E_G + 2\delta_0/3} \times \int_0^\infty dk k^2 \left(E_G + \frac{\hbar^2 k^2}{2\mu} \right)^2 f_k^{e,h}, \quad (4)$$

where ϵ_r is the average dielectric constant of the host semiconductor. It is clear from Eq. (4) that the greater the band gap or the higher the carrier temperature, the stronger the power-loss density will be.

The formula for the absorption power in the third step can be derived from a perturbative linear-response theory [7,8] by inserting an interband transition energy. In this way, the expression for the stimulated-transition rate changes to that for the power-density gain. The power-density gain due to three-photon nonlinear excitation by a spatially uniform electromagnetic field for $3\hbar\Omega_p \geq E_G > \hbar\Omega_p$ is [7,8,16]

$$\mathcal{W}_{\text{ab}} = \frac{2}{\pi^2 \hbar} \int_0^\infty dk k^2 \Delta_1^2(k) \left(E_G + \frac{\hbar^2 k^2}{2\mu} \right) \times \frac{\gamma_0 (1 - f_k^e - f_k^h)}{\gamma_0^2 + (E_G + \hbar^2 k^2 / 2\mu - 3\hbar \Omega_p)^2}, \quad (5)$$

where [8]

$$\Delta_1^2(k) = \frac{2\Delta_R^4}{(E_G + \hbar^2 k^2 / 2\mu)^2 - \hbar^2 \Omega_p^2}, \quad (6)$$

and γ_0 is the homogeneous level broadening due to the finite lifetime of quasiparticles.

Equation (1) above describes the first step of a coherent three-photon laser pumping with nonequilibrium distributions of electrons and holes in the absence of carrier scattering and photoluminescence. It is a result of the balance between the optical gain and the optical absorption. There is no homogeneous level broadening from electron scattering in this case. On the other hand, Eq. (5) describes the third step, during which a nonlinear optical absorption process occurs with quasiequilibrium distributions of electrons and holes in the presence of ultrafast carrier scattering. In this case, there

is a homogeneous level broadening due to the quasiparticle lifetime from the Coulomb scattering of carriers. It is seen from Eq. (6) that the greater the excitation-field amplitude is, the higher the power-gain density will be. For simplicity, we do not include recapture of photons of photoluminescence here by assuming a unit escape probability. We would like to point out that the carrier-phonon system cannot be simply treated as a blackbody system because of the existence of net energy exchange between carrier and phonons when the carrier and lattice temperatures are different. As a result, the Einstein relation between optical absorption and spontaneous emission [21,22] cannot be applied in this situation even though the Fermi-Dirac and Bose-Einstein functions are assumed for carriers and phonons, respectively.

The formula for the energy exchange in the third step between carriers and phonons and between carriers and impurities by including the assisted photon absorption can be obtained from the balance equation [see [23] and Ref. [14] therein]. By keeping only the leading order interaction between electrons and phonons or impurities, we get the power-exchange density $\mathcal{W}_{\text{ex}}^\alpha$ for impurities, phonons, and assisted photon emission or absorption [23,24]:

$$\begin{aligned} \mathcal{W}_{\text{ex}}^\alpha = & \frac{n_i}{2\pi^3} \int_0^\infty dq q^2 |U_{\text{imp}}^\alpha(q)|^2 \sum_{n=-\infty}^\infty \left[J_n \left(\frac{eq\mathcal{E}_p}{\sqrt{2}m_\alpha^* \Omega_p} \right) \right]^2 n \Omega_p \int_0^\infty dk k^2 (f_k^\alpha - f_{|k+q|}^\alpha) \delta(E_{|k+q|}^\alpha - E_k^\alpha - n\hbar\Omega_p) \\ & - \frac{\mathcal{V}}{\pi^3} \sum_\lambda \int_0^\infty dq q^2 |C_{q\lambda}^\alpha|^2 \sum_{n=-\infty}^\infty \left[J_n \left(\frac{eq\mathcal{E}_p}{\sqrt{2}m_\alpha^* \Omega_p} \right) \right]^2 (\omega_{q\lambda} - n\Omega_p) \left[N_0 \left(\frac{\hbar\omega_{q\lambda}}{k_B T_L} \right) - N_0 \left(\frac{\hbar\omega_{q\lambda} - n\hbar\Omega_p}{k_B T_\alpha} \right) \right] \\ & \times \int_0^\infty dk k^2 (f_k^\alpha - f_{|k+q|}^\alpha) \delta(E_{|k+q|}^\alpha - E_k^\alpha + \hbar\omega_{q\lambda} - n\hbar\Omega_p), \end{aligned} \quad (7)$$

where $\alpha=e$ ($\alpha=h$) for electrons (holes), \mathcal{V} is the sample volume, $E_k^\alpha = \hbar^2 k^2 / 2m_\alpha^*$ is the kinetic energy, T_L is the lattice temperature, and T_e (T_h) is the electron (hole) temperature. In Eq. (7), the higher-order vertex correction from the ladder diagrams to the density-density correlation function has been neglected at high electron temperatures. Moreover, unpolarized incident light is assumed, $N_0(x) = [\exp(x) - 1]^{-1}$ is the Bose-Einstein function, n is an integer, $J_n(x)$ is the n th-order Bessel function, $\hbar\omega_{q\lambda}$ is the phonon energy for phonon wave number q and mode λ , n_i is the impurity concentration, $U_{\text{imp}}^\alpha(q) = e^2 / [\epsilon_0 \epsilon_r (q^2 + \Lambda_\alpha^2)]$ is the electron-impurity interaction, $1/\Lambda_\alpha$ is the Thomas-Fermi screening length [17,18], and $|C_{q\lambda}^\alpha|^2$ is the carrier-phonon coupling strength. For polar semiconductors, such as $\text{Al}_x\text{Ga}_{1-x}\text{N}$, there exist both acoustic and optical phonon modes. For optical phonon modes, only the longitudinal-optical phonon mode can strongly couple to electrons and the coupling strength can be obtained from the Fröhlich electron-phonon coupling model [17,18]. For acoustic phonon scattering, on the other hand, we use the deformation-potential approximation [17,18]. It is clear from

Eq. (7) that the carrier energy loss or gain from phonons under an excitation field depends on whether the carrier temperature is higher or lower than the lattice temperature, respectively.

In order to cool the lattice, the power gain of carriers due to the excitation field must be smaller than the power loss due to spontaneous photon emission. This requires a weak excitation field \mathcal{E}_p and a large band gap E_G . As a result of weak excitation, the concentration of conduction electrons is very low. The carriers gain power from the excitation field but lose power through the spontaneous photon emission. In addition, they exchange power with phonons and assisted photons. Thus energy conservation in steady state requires [6]

$$\mathcal{W}_{\text{ab}} - \mathcal{W}_{\text{sp}} + \mathcal{W}_{\text{ex}}^e + \mathcal{W}_{\text{ex}}^h = 0. \quad (8)$$

The detailed balance between strongly interacting electrons and holes for any given lattice temperature gives rise to a uniform carrier temperature ($T_e = T_h$) [25].

The previous local energy-balance equation is a rate-type equation [22,26]. It neglects the change of the carrier distribution when the temperature of the system is lowered. On the other hand, our generalized nonlocal energy-balance equation for linear excitation has included the dynamical change of the carrier distributions when the temperature of the system decreases with time [6]. The solution of a generalized nonlocal energy-balance equation provides the carrier temperature for any given lattice temperature T_L . Equation (8) implies that the larger the value of $|\mathcal{W}_{ab}-\mathcal{W}_{sp}|$, the greater the deviation of T_e will be from T_L .

Electrons stay in a quasiequilibrium state with T_e due to pair scattering. The electron temperature is affected by the electron-phonon scattering. Although the phonons also stay in a quasiequilibrium state, the phonon temperature T_L directly evolves with time due to an imbalance between the power loss to electrons and holes and the power gain from any thermal source (such as the background thermal radiation). As a result, the average phonon energy varies with time. This gives rise to [6]

$$\begin{aligned} & \frac{\hbar^2}{8\pi^2 k_B T_L^2} \left(\frac{dT_L}{dt} \right) \sum_{\lambda} \int_0^{q_D^{\lambda}} dq q^2 \omega_{q,\lambda}^2 \sinh^{-2} \left(\frac{\hbar \omega_{q,\lambda}}{2k_B T_L} \right) \\ &= \frac{\sigma A_s}{\mathcal{V}} (T_B^4 - T_L^4) - (\mathcal{W}_{ex}^e + \mathcal{W}_{ex}^h) \\ &= \frac{\sigma A_s}{\mathcal{V}} (T_B^4 - T_L^4) - (\mathcal{W}_{sp} - \mathcal{W}_{ab}), \end{aligned} \quad (9)$$

where q_D^{λ} is the Debye wave number for phonons in the λ mode, $\sigma = \pi^2 k_B^4 / 60 \hbar^3 c^2$ is the Stefan-Boltzmann constant, and A_s is the surface area of the sample. We assume $T_L = T_0$ at $t=0$; T_0 is the initial temperature of equilibrium phonons, and T_B is the environmental temperature which approaches T_0 for band-edge excitation with very weak field. The first term on the right-hand side of Eq. (9) is much smaller than the second term even when $T_L \neq T_B$. The rate of reduction of T_L is determined by $\mathcal{W}_{ex}^e + \mathcal{W}_{ex}^h$, which decreases with decreasing T_L , and the temperature difference $T_L - T_e$. Moreover, the dependence of E_G on T_L will be neglected for wide-band-gap semiconductors such as $Al_xGa_{1-x}N$. From Eq. (9) we know that the laser cooling of the lattice implies $\mathcal{W}_{ex}^e + \mathcal{W}_{ex}^h > 0$. This requires $\mathcal{W}_{sp} - \mathcal{W}_{ab} > 0$ in steady state. This can be satisfied only for large E_G and weak \mathcal{E}_p .

In this paper, we only provide the formulas for the laser cooling of the lattice of a semiconductor in the case of three-photon nonlinear excitation. The related expressions for the case of linear excitation can be found in our previous work [6].

III. NUMERICAL RESULTS AND DISCUSSION

In this paper, we consider the semiconductor $Al_xGa_{1-x}N$ for our numerical calculations, where x is the percentage of Al in the alloy. For AlN, we choose the following parameters: $E_G = 6.2$ eV, $m_e^*/m_0 = 0.4$, $m_h^*/m_0 = 3.53$, $\delta_0 = 0.019$ eV. The static dielectric constant is $\epsilon_s = 8.5$. The high-frequency dielectric constant is $\epsilon_{\infty} = 4.77$. The LO phonon energy is

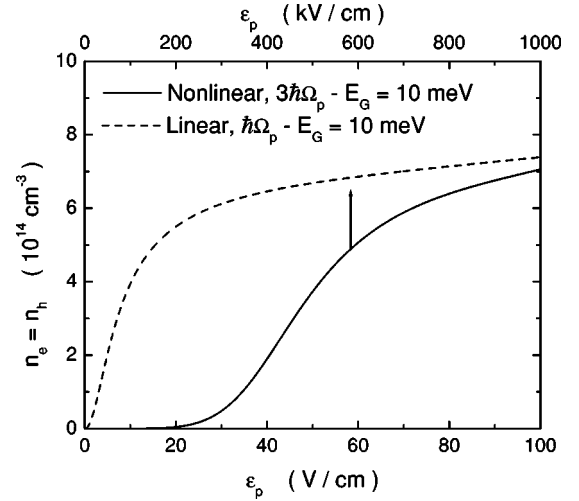


FIG. 1. Calculated excited carrier density $n_e = n_h$ for AlN as a function of amplitude of excitation field \mathcal{E}_p for three-photon nonlinear (solid curve with upper and left scales) and linear (dashed curve with lower and left scales) excitation. Here, $\hbar\Omega - E_G = 10$ meV with $\Omega = 3\Omega_p$ for three-photon nonlinear excitation and $\Omega = \Omega_p$ for linear excitation. The other parameters are given in the text.

$\hbar\omega_{LO} = 99.2$ meV. The ion mass density is $\rho = 3.23$ g/cm³. The deformation-potential coefficient is $D = -9.5$ eV and the piezoelectric constant is $h_{14} = 6.9 \times 10^7$ V/cm. The transverse sound velocity is $c_t = 3.7 \times 10^5$ cm/s and the longitudinal sound velocity is $c_l = 9.12 \times 10^5$ cm/s. The Debye wave number is $q_D^{\lambda} = (48\pi^2)^{1/3} / a_0$ with $a_0 = 3.57$ Å, $n_i = 10^{10}$ cm⁻³, $\epsilon_t = (\epsilon_s + \epsilon_{\infty}) / 2$, the sample is assumed to be cubic with an edge size of 1 cm, and $\gamma_0 = \hbar / \tau$ with $\tau = 0.1$ ps. The other parameters, such as \mathcal{E}_p , $3\hbar\Omega_p - E_G$, and T_0 , will be given in the figure captions.

Figure 1 displays the calculated excited carrier concentration $n_e = n_h$ for AlN as a function of the excitation-field strength \mathcal{E}_p . From the figure we observe that there exists a saturation of carrier concentration when \mathcal{E}_p is really large for both linear (dashed curve) and three-photon nonlinear (solid curve) excitation. However, there exists a threshold value for \mathcal{E}_p for three-photon nonlinear excitation. This is attributed to the energy-dependent broadening effect in Eq. (1) whose broadening expression is given explicitly in Eq. (2).

Figure 2 presents the calculated excited carrier concentration $n_e = n_h$ for AlN as a function of the field-frequency detuning $\hbar\Omega - E_G$ for linear ($\Omega = \Omega_p$ and dashed curve) and three-photon nonlinear ($\Omega = 3\Omega_p$ and solid curve). From the figure, we easily find that the excitation efficiency is higher for linear excitation with $\mathcal{E}_p = 10$ V/cm compared to that of three-photon nonlinear excitation with $\mathcal{E}_p = 500$ kV/cm. For both cases, there exists a relationship $n_e = n_h \propto \sqrt{\hbar\Omega - E_G}$.

Figure 3 shows the calculated power-exchange density $\mathcal{W}_{ex} = \mathcal{W}_{ex}^e + \mathcal{W}_{ex}^h$ for AlN with three-photon nonlinear excitation as a function of time t for three values of $\mathcal{E}_p = 50$ V/cm (dashed curve with upper and right scales), 80 V/cm (solid curve), and 95 V/cm (dash-dotted curve). Here, $3\hbar\Omega_p - E_G = 10$ meV and $T_0 = 300$ K. When $\mathcal{E}_p = 50$ V/cm, positive \mathcal{W}_{ex} implies the laser cooling of the lattice. However, the change of \mathcal{W}_{ex} is very slow for this case

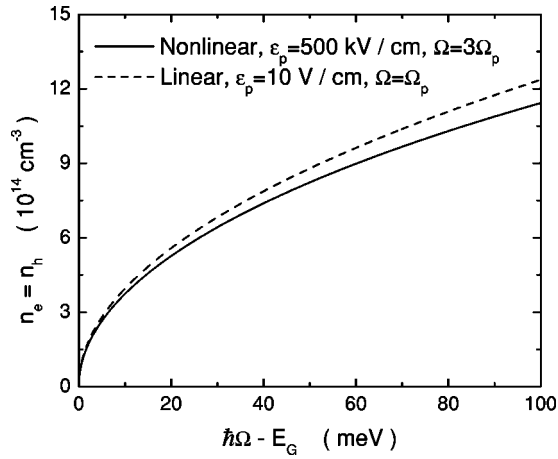


FIG. 2. Calculated excited carrier density $n_e = n_h$ for AlN as a function of detuning of excitation-field frequency $\hbar\Omega - E_G$ for three-photon nonlinear (solid curve) and linear (dashed curve) excitation. Here, $\mathcal{E}_p = 10$ V/cm, $\Omega = \Omega_p$ for linear excitation, and $\mathcal{E}_p = 500$ kV/cm, $\Omega = 3\Omega_p$ for three-photon nonlinear excitation. The other parameters are given in the text.

(larger time scale). When \mathcal{E}_p is increased to 80 V/cm, we find that the laser cooling of the lattice significantly decreases with time. When \mathcal{E}_p is further increased to 95 V/cm, a negative \mathcal{W}_{ex} implies the laser heating of the lattice. But the change of \mathcal{W}_{ex} is still small.

Figure 4 demonstrates the calculated power-exchange density $\mathcal{W}_{\text{ex}} = \mathcal{W}_{\text{ex}}^e + \mathcal{W}_{\text{ex}}^h$ for AlN with three-photon nonlinear excitation and $\mathcal{E}_p = 80$ V/cm as a function of time t for three different cases. The first case corresponds to $3\hbar\Omega_p - E_G = 10$ meV and $T_0 = 300$ K (solid curve with lower and left scales). The second case corresponds to $3\hbar\Omega_p - E_G = 20$ meV and $T_0 = 300$ K (dashed curve). The third case corresponds to $3\hbar\Omega_p - E_G = 10$ meV and $T_0 = 77$ K (dash-dotted curve). When the field-frequency detuning $3\hbar\Omega_p - E_G$ is increased from 10 to 20 meV (comparing case 1 with case 2), the positive

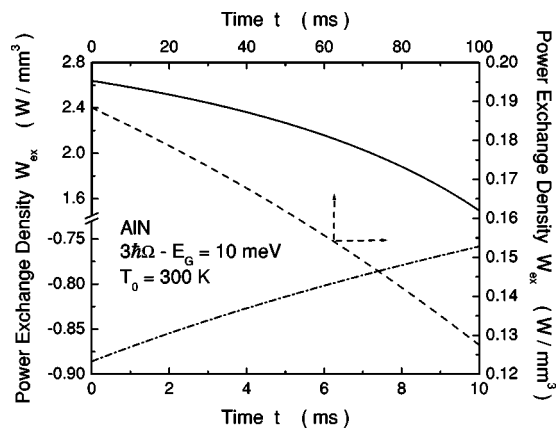


FIG. 3. Calculated power-exchange density $\mathcal{W}_{\text{ex}} = \mathcal{W}_{\text{ex}}^e + \mathcal{W}_{\text{ex}}^h$ for AlN as a function of time t with three-photon nonlinear excitation, $3\hbar\Omega_p - E_G = 10$ meV and $T_0 = 300$ K for three different cases. These cases include $\mathcal{E}_p = 50$ V/cm (dashed curve with upper and right scales); $\mathcal{E}_p = 80$ V/cm (solid curve with lower and left scales); and $\mathcal{E}_p = 95$ V/cm (dash-dotted curve with lower and left scales). The other parameters are given in the text.

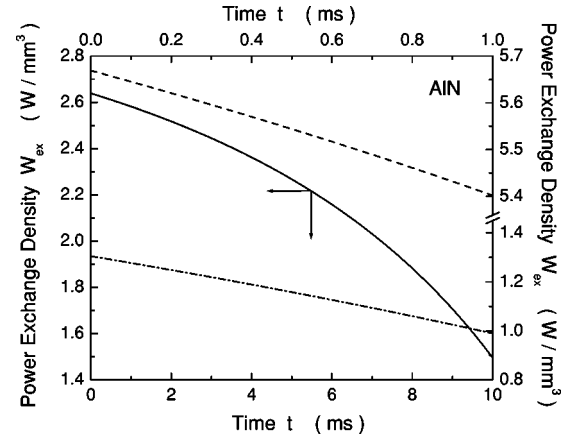


FIG. 4. Calculated power-exchange density $\mathcal{W}_{\text{ex}} = \mathcal{W}_{\text{ex}}^e + \mathcal{W}_{\text{ex}}^h$ for AlN as a function of time t with three-photon nonlinear excitation and $\mathcal{E}_p = 80$ V/cm for three different cases. These cases include $3\hbar\Omega_p - E_G = 10$ meV and $T_0 = 300$ K (solid curve with lower and left scales); $3\hbar\Omega_p - E_G = 20$ meV and $T_0 = 300$ K (dashed curve with upper and right scales); and $3\hbar\Omega_p - E_G = 10$ meV and $T_0 = 77$ K (dash-dotted curve with upper and right scales). The other parameters are given in the text.

\mathcal{W}_{ex} increases due to higher excited carrier concentration. When the initial lattice temperature T_0 decreases from 300 to 77 K (comparing case 1 with case 3), the positive \mathcal{W}_{ex} is reduced.

Figure 5 exhibits the calculated power-exchange density $\mathcal{W}_{\text{ex}} = \mathcal{W}_{\text{ex}}^e + \mathcal{W}_{\text{ex}}^h$ for AlN with linear excitation, $\hbar\Omega_p - E_G = 10$ meV, and $T_0 = 300$ K as a function of time t for two values of $\mathcal{E}_p = 25$ V/cm (dashed curve with upper scale) and 90 V/cm (solid curve with lower scale). \mathcal{W}_{ex} for the case of linear excitation is two orders of magnitude larger than \mathcal{W}_{ex} for the case of three-photon nonlinear excitation. Moreover, the change of \mathcal{W}_{ex} with time for linear excitation is three

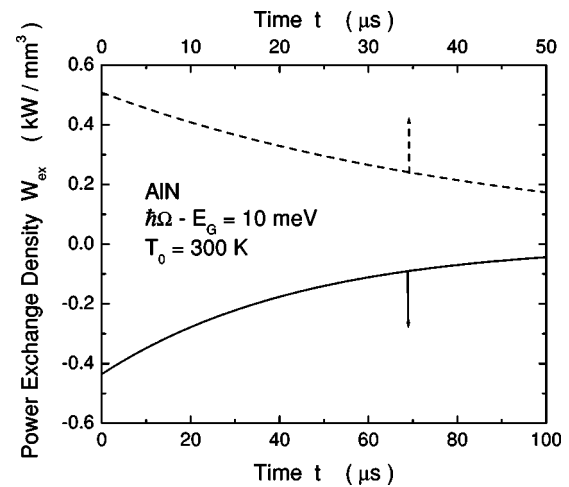


FIG. 5. Calculated power-exchange density $\mathcal{W}_{\text{ex}} = \mathcal{W}_{\text{ex}}^e + \mathcal{W}_{\text{ex}}^h$ for AlN as a function of time t with linear excitation, $\hbar\Omega_p - E_G = 10$ meV, and $T_0 = 300$ K for two different cases. These two cases include $\mathcal{E}_p = 25$ V/cm (dashed curve with upper and left scales); and $\mathcal{E}_p = 90$ V/cm (solid curve with lower and left scales). The other parameters are given in the text.

orders of magnitude faster than that for three-photon nonlinear excitation. When \mathcal{E}_p increases from 25 to 90 V/cm, the laser cooling of the lattice changes to laser heating. Finally, by comparing Fig. 5 with Fig. 3, we find that the curvature of the cooling curves shows opposite signs. This implies that the reduction of the power-exchange density for laser cooling of the lattice is sublinear in linear excitation, but it is superlinear in three-photon nonlinear excitation. Unfortunately, we have to use laser fields with ultraviolet frequencies to excite carriers in the linear excitation case.

IV. CONCLUSIONS

By using a generalized nonlocal energy-balance equation for excited carriers and phonons, we have demonstrated laser

cooling of the lattice of the wide-band-gap semiconductor AlN using a He-Ne laser through three-photon nonlinear excitation process. We have compared the power-exchange densities of the system, which produce laser cooling of the lattice when they are positive, with different strengths of the laser field. We have also studied the effects of initial lattice temperature and field-frequency detuning on the laser cooling of the lattice. Finally, we have compared the power-exchange densities for both laser cooling and heating in linear excitation and three-photon nonlinear excitation. Our calculation has shown that linear excitation seems more favorable than three-photon nonlinear excitation for laser cooling of the lattice of a wide-band-gap semiconductor. However, resonant three-photon nonlinear absorption allows us to use a He-Ne laser for laser cooling of the lattice of AlN.

-
- [1] P. Pringsheim, *Z. Phys.* **57**, 739 (1929).
 - [2] H. Gauck, T. H. Gfroerer, M. J. Renn, E. A. Cornell, and K. A. Bertness, *Appl. Phys. A: Mater. Sci. Process.* **64**, 143 (1997).
 - [3] G. Lei, J. E. Anderson, M. I. Buchwald, B. C. Edwards, R. I. Epstein, M. T. Murtagh, and G. H. Sigel, Jr., *IEEE J. Quantum Electron.* **34**, 1839 (1998).
 - [4] B. C. Edwards, J. E. Anderson, R. I. Epstein, G. L. Mills, and A. J. Mord, *J. Appl. Phys.* **86**, 6489 (1999).
 - [5] J. Fernandez, J. A. Mendioroz, A. J. Garca, R. Balda, and J. L. Adam, *Phys. Rev. B* **62**, 3213 (2000).
 - [6] D. H. Huang, T. Apostolova, P. M. Alsing, and D. A. Cardimona, *Phys. Rev. B* **70**, 033203 (2004).
 - [7] P. M. Alsing, D. H. Huang, D. A. Cardimona, and T. Apostolova, *Phys. Rev. A* **68**, 033804 (2003).
 - [8] Y. R. Shen, *The Principles of Nonlinear Optics* (Wiley, New York, 1984).
 - [9] R. Cingolani *et al.*, *Phys. Rev. Lett.* **69**, 1276 (1992).
 - [10] Leung Tsang *et al.*, *Phys. Rev. B* **41**, 5942 (1990), and references therein.
 - [11] J. Khurgin *et al.*, *Appl. Phys. A: Solids Surf.* **53**, 523 (1991), and references therein.
 - [12] M. Lindberg and S. W. Koch, *Phys. Rev. B* **38**, 3342 (1988); J. V. Moloney, R. A. Indik, J. Hader, and S. W. Koch, *J. Opt. Soc. Am. B* **16**, 2023 (1999).
 - [13] K. Meissner, B. Fluegel, H. Gießen, B. P. McGinnis, A. Paul, R. Binder, S. W. Koch, N. Peyghambarian, M. Grün, and C. Klingshirn, *Phys. Rev. B* **48**, 15472 (1993).
 - [14] S. Schmitt-Rink, D. S. Chemla, and H. Haug, *Phys. Rev. B* **37**, 941 (1988).
 - [15] S. Adachi, *J. Appl. Phys.* **53**, R1 (1985).
 - [16] G. D. Mahan, *Phys. Rev.* **153**, 882 (1967).
 - [17] T. Apostolova, D. H. Huang, P. M. Alsing, J. McIver, and D. A. Cardimona, *Phys. Rev. B* **66**, 075208 (2002).
 - [18] D. H. Huang, P. M. Alsing, T. Apostolova, and D. A. Cardimona, *Phys. Rev. B* **69**, 075214 (2004).
 - [19] D. H. Huang and S. K. Lyo, *Phys. Rev. B* **59**, 7600 (1999).
 - [20] D. H. Huang and D. A. Cardimona, *Phys. Rev. A* **64**, 013822 (2001).
 - [21] H. Haug and S. Schmitt-Rink, *J. Opt. Soc. Am. B* **2**, 1135 (1985).
 - [22] L. A. Rivlin and A. A. Zadernovsky, *Opt. Commun.* **139**, 219 (1997).
 - [23] X. L. Lei, *J. Appl. Phys.* **84**, 1396 (1998).
 - [24] A. Kaiser, B. Rethfeld, H. Vicanek, and G. Simon, *Phys. Rev. B* **61**, 11437 (2000).
 - [25] Jianzhong Li and C. Z. Ning, *Phys. Rev. A* **66**, 023802 (2002).
 - [26] A. N. Oraevsky, *J. Russ. Laser Res.* **17**, 471 (1996).